Derivation and analysis of a state-space model for transient control of liquid-propellant rocket engines

Sergio Pérez-Roca
CNES
and ONERA
Paris area, France
e-mail: sergio.perez_roca@onera.fr

Julien Marzat, Hélène Piet-Lahanier
DTIS
ONERA, Université Paris-Saclay
Palaiseau, France
e-mail: julien.marzat@onera.fr, helene.piet-lahanier@onera.fr

Nicolas Langlois
Normandie Université, UNIROUEN
ESIGELEC, IRSEEM
Rouen, France
e-mail: nicolas.langlois@esigelec.fr

Marco Galeotta, François Farago
Direction des Lanceurs
CNES
Paris, France
e-mail: marco.galeotta@cnes.fr, francois.farago@cnes.fr

Serge Le Gonidec
JTIL, JOLE 1
ArianeGroup SAS
Vernon, France
e-mail: serge.le-gonidec@ariane.group

***Abstract*—A dynamic model of a liquid-propellant rocket engine has been developed in this paper, with the future purpose of meeting the more demanding requirements of rocket-engines control forced by the new reusability scenarios. This transient-representative modelling approach has been carried out in two phases: initially the purely thermodynamic modelling and subsequently its adaptation to the control framework. The former was tackled by building first a representative simulator of the well-known *Vulcain* engine. The differential equations considered come from mass, momentum and energy conservation equations and from turbo-pump dynamics. In general, macroscopic behaviour at component and system levels is considered. Once this simulator started to provide satisfactory results, it was translated into a state-space model for control by symbolically joining all components' equations, which led to a set of differential equations capturing system's global behaviour. Its states consist in mass flows, pressures, temperatures and shaft rotational speeds. The available actuators are five continuously-controllable valves, one binary igniter and one binary starter. That combination of continuous and discrete features forces the definition of a hybrid system in the control sense. The analysis of its dynamic characteristics points to a good controllability of thrust via the gas-generator injection valves, and of mixture ratio via the turbines' flow-distribution valve.**

***Index Terms*—Liquid-propellant rocket engine, nonlinear modelling & control, reusability, robust control, thermodynamics, transient behaviour, hybrid systems.**

I. Introduction

The current trend towards a more affordable access to space is generally materialising in reusable launchers and hence in reusable engines. In Europe, new studies on these engines are being performed within the framework of the *Prometheus* engine project. From the control perspective, these reusable engines imply more demanding robustness requirements than expendable ones, mainly because of their multi-restart and thrust-modulation capabilities.

The classical steady-state multivariable and linear control of liquid-propellant rocket engines (LPRE) has attained a reduced throttling envelope, between 70% and 120% of nominal thrust [1]. One of the objectives of current research programmes is to enlarge that envelope in order to face reusability scenarios by means of an adequate model. Indeed, the modelling approach in this paper combines elements from purely thermodynamic modelling for simulation and from modelling for control. In the literature, one can find different ways of representing an engine for control purposes.

Some authors opted for identifying the system due to its complexity, such as [2], devoted to the staged-combustion SSME (Space Shuttle Main Engine). They considered an open loop with the opening angle of its main five valves as inputs, and eight outputs, comprising pressures, temperatures and speeds of both turbines. Preliminary information on the system's nonlinearities and bandwidths was obtained by exciting the open and closed loops. The initial models of *Vinci* in [3] come from an accurate simulator and hence contain around forty states concerning pumps, turbines, shafts, adiabatic pipes, regenerative circuit, orifices, cavities and combustion chambers. Then it is reduced to a 5-state one, whose parameters are identified thanks to the simulator. Other authors reviewed do not rely on identification techniques for deriving their engine model. Regarding the reusable engine modelling by [4] or [5], similar to the SSME, standard lumped parameter schemes have been applied for approximating the partial differential equations related to mass, momentum and energy conservation, the main equations in thermo-fluid-dynamic modelling, as first-order ones. Causal interconnections (as in CARINS software by CNES and ONERA [6]) are defined to join all the engine's

sub-elements, which results in a plant model of eighteen states, two control inputs and two outputs. However, the model is linearised around the steady-state and reduced to a 13-state model via the HANKEL order reduction. In another paper by those authors [7], it is claimed that the linear models of that engine did not present relevant variations while throttling.
In [8], describing functions (DF) are used instead of full models, being capable of dealing with nonlinear and time-varying systems of equations at a satisfactory robustness level. Concretely, sinusoidal-input DF (SIDF) models are employed, which require a sinusoidal excitation of the plant and the computation of FOURIER integrals of nonlinear equations.
References [9] and [10] present a model block diagram in the frequency domain for a generic LPRE. The components described in those papers are the combustion chamber, the injector head, cooling jacket and pipelines, which are modelled linearly and at the nominal operating regime.
The engine model used in [11], based on nonlinear mass, heat and power equations, comprises four turbopumps, three combustors, two multiphase heat exchangers, a nozzle and pipes, adding up to forty states.
A performance model simulating *Vulcain*'s internal flow characteristics (pressure, temperature and flow rate) was developed in [12] and is very close to the one in this paper. The main input data to the model are pump-inlet pressures and temperatures, geometric and thermal features and valve settings. Twelve unknowns are considered: thrust chamber and gas-generator (GG) mass flows, dump-cooling mass flow, pumps rotational speed, turbine-outlet pressures and temperatures and H_2-turbine mass flow. Engine parameters are obtained by data reconciliation with tests, that is to say, by estimation through generalised sum of residual squares.
Reference [13] applied the state-space framework to the analysis of the dynamic characteristics of a variable thrust LPRE. The engine concerned presents a pressure-fed cycle, whose coaxial injector's cross sections can be controlled by varying the displacement of their pintles. The feedback signal is the measured combustion pressure times a gain. Seven states are selected for the model: chamber pressure, gas mixture ratio, injected mass flows, and pintle's displacement and velocity.
Regarding the way of building a thermodynamic simulator, it is relevant to mention the only open-source *MATLAB® /Simulink®* toolbox for modelling and analysis of thermodynamic systems (*T-MATS*) until the date [14]. *T-MATS* includes several thermodynamic and control modelling libraries, with focus on gas turbines. In other words, a complete system simulation can be set up by joining 0-D thermodynamic component models. The enhanced *T-MATS-Cantera* sub-library [15] allows the computation of precise fluid properties according to the thermodynamic state and chemical composition.

A. Objectives and outline

The objectives of this paper are basically two-fold. Firstly, a representative yet simple thermodynamic simulator of a LPRE, capturing its transient behaviour, was sought. Secondly, it was also aimed at deriving a symbolic state-space model of the same engine, that is to say, a set of nonlinear ordinary differential equations (ODEs).
Indeed, the broader goal is to enhance the control of pump-fed LPRE in general, the main target being their usually damaging transient phases (start-up, shutdown, throttling), currently carried out as event sequences in open loop. The aforementioned two ways of modelling the system consist in crucial blocks of that broader control loop under elaboration. The former will represent the real plant at a certain degree of accuracy, and the latter will serve for carrying out model-based control approaches.
Due to the need for an enlarged operating domain, to quick variations during transients and to the natural nonlinearity of thermo-fluid-dynamic equations, models in this paper are nonlinear. They capture the varying dynamics corresponding to configuration changes driven by sequential-logical events (valves opening, main chamber ignitions or starter activations). The main target in this study is a GG cycle because *Prometheus*, the potential engine application of these studies, is of this type.
However, the intention is to also consider other engines and cycles so as to obtain a method globally applicable to rocket engines. The main quantities which are usually controlled are combustion chamber's pressure, which is related to engine's thrust; and propellant mixture ratio, related to temperature. Hence, the modelling of their transient evolution has been studied so as to enable the future controller to predict them better and consequently to obtain more satisfactory performance results in a robust way.
Section II is devoted to introducing the *Vulcain* engine, the one selected for deriving its model. Section III presents the thermo-fluid-dynamic modelling formulation in a component-wise way, generic to rocket engines. Section IV is devoted to translate the *Vulcain* purely thermodynamic simulator into a formal state-space model for control purposes. Finally, results are presented and analysed in Section V.

II. VULCAIN ENGINE DESCRIPTION

The engine case study is the retired *Vulcain* 1 (*ArianeGroup* 1996-2009) since it corresponds to a well-known gas-generator cycle in Europe from which test-campaigns data are available. The main approximate steady-state operating data of this Ariane 5 main stage engine are summarised in Table I. For the sake of clarity, the real schematic of this engine is presented in fig. 1. In that figure the main components of the engine are depicted. Most importantly, it consists in a LOX/LH_2 (liquid oxygen as oxidiser, liquid hydrogen as fuel) engine, which forces the use of two different turbopumps to pump propellants from tanks due to their high density difference. The hot-gas flow necessary to drive turbines comes from a gas generator, which is a small combustion chamber that receives a small portion of propellants main flow. The actuators considered in this paper are five continuously-controllable valves (VCH, VCO, VGH, VGO and VGC), one binary igniter (i_{CC}) and one binary starter (i_{GG}).
H stands for hydrogen, O for oxygen, CC or C for combustion

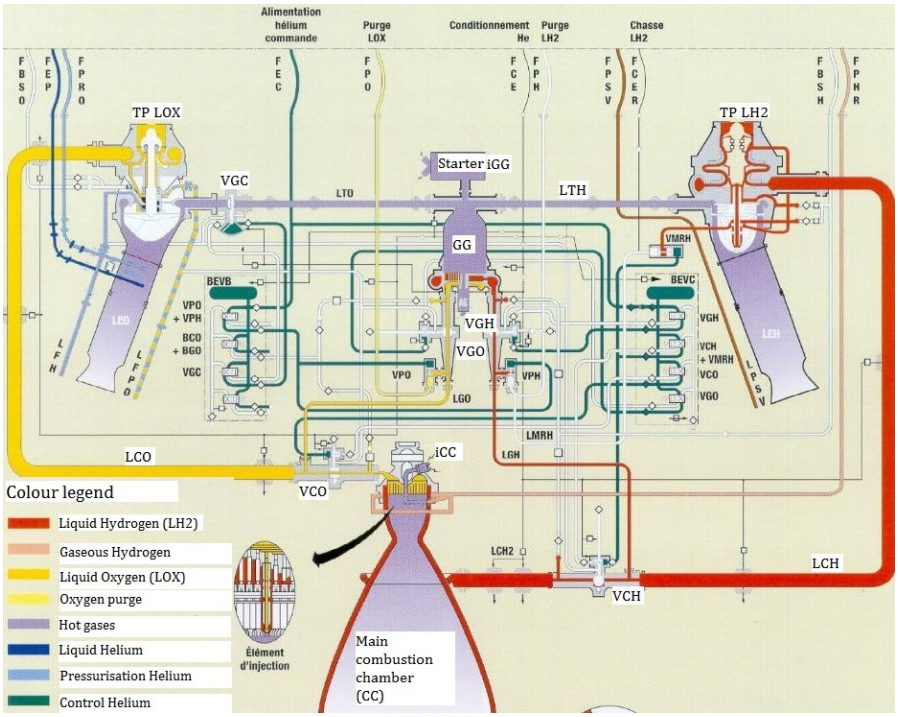

Fig. 1. Schematic of the Vulcain engine by ArianeGroup and CNES

chamber, GG or G for gas generator, V for valve, GC for hot gases, I for igniter/starter, L for line, T or turbine, PF for fuel pump and PO for oxidiser pump.

Valves angles (α) control the flows to the main combustion chamber (VCH and VCO), where thrust is produced thanks to the high pressure attained ($100bar$); to the gas generator (VGH, VGO), and to the oxidiser turbine (VGC). The latter consists in the main contribution in determining mixture ratio (MR), which is defined as the quotient between oxidiser and fuel mass flow rates:

$$MR = \frac{\dot{m}_{ox}}{\dot{m}_{fu}}. \tag{1}$$

This ratio is defined at three levels: at an engine's global level (MR_{PI}), taking pumped propellants into account; in the combustion chamber (MR_{CC}) and in the gas generator (MR_{GG}). Chamber's igniter i_{CC} enables combustion in that cavity and gas-generator's starter i_{GG} injects hot gas into that cavity during less than $1.5s$ so as to start driving turbines. This consists in the main contribution to start-up, because once turbines start rotating, pumps can provide more flow to chambers, which increases combustion pressures and temperatures. These increases also lead to greater shaft speeds until a steady-state is achieved, at around three to four seconds after start.

Tanks contain propellants at assumed constant cryogenic conditions: $3bar$ and $21K$ in the hydrogen case and at $7bar$ and $90K$ in the oxygen one. Not all the elements depicted in fig. 1 are going to be considered in this paper. Only the core system lies within the scope because it represents the dominant behaviour of the engine. Hence, all subsystems such as Helium lines are ignored. It seems relevant to summarise the flow paths and elements considered in this paper:

- Hydrogen line: the hydrogen leaving the tank is absorbed by pump PH, which pumps it to valves through a common pipe LCH. After this pipe, flow is split into the combustion-chamber valve VCH and the gas-generator valve VGH. In VCH, the resistance contribution of the cooling circuit, affecting fuel flow before the main chamber, is taken into account.
- Oxygen line: same path as hydrogen (oxygen tank, PO, LCO, then split into VCO and VGO), but it does not flow through the cooling circuit.
- Hot gases: the mixtures of oxygen and hydrogen are burned at independent ratios (determined by valves) in the two chambers CC and GG. The output flow of CC

TABLE I
Vulcain 1 STEADY-STATE OPERATING DATA

Parameter	Value
Chamber mixture ratio	5.9
Gas-generator mixture ratio	$[0.9, 1]$
Thrust (vacuum)	$1025kN$
Thrust (ground)	$815kN$
Chamber pressure	$100bar$
Gas-generator pressure	$87bar$
Chamber temperature	$3500K$
Gas-generator temperature	$1000K$
Turbopumps rotational speed (LOX)	$[11000, 14800]rpm$
Turbopumps rotational speed (LH2)	$[28500, 36000]rpm$

is discharged into the atmosphere through a converging-diverging nozzle. Nevertheless, the diverging part of the nozzle is not considered in this paper since it does present a direct impact on chamber's pressure, one of the main variables to control.
GG output is split into two lines, one for each turbine. The path to the hydrogen turbine TH is performed through the pipe LTH, and the path to the oxygen turbine TO crosses the valve VGC. Turbines exhaust is directly emitted to the atmosphere too. These turbines are obsviously mechanically connected to their respective pumps by means of shafts.

III. Thermo-fluid-dynamic modelling

A simple, dynamic and efficient way of modelling generic LPRE is sought, instead of using more accurate programmes or computations. An easy integration into *Simulink*® is also preferred so as to test different control methods in the future. Along these lines, a new *Simulink*® library of rocket-engine components has been developed to build the simulator in this paper. It has been named *T-RETM*, Toolbox for Rocket-Engine Transient Modelling. It is slightly based on components from *T-MATS Cantera* [15], which was not completely adequate to this case due to some limitations. For instance, it is conceived for jet engines, does not present thermodynamic differential equations (only a mechanic ODE on shaft's speed) and requires relatively long computational times.

A. Model formulation

The following paragraphs describe the equations, assumptions and conditions considered in the models of all main components, presented in order of fluid flow in the *Vulcain* engine. In general, gases are considered semi-perfect or thermally-perfect, since the ideal-gas law is assumed but their caloric properties are temperature-dependent.
There is a fluid flow vector or set of thermodynamic and chemical variables shared between connected 0-D components. Its twelve elements are mass flow, total conditions (temperature, pressure, enthalpy, density), specific heat ratio and composition. In the following, thermodynamic variables will be referenced to these total quantities even when omitting the adjective. All units are SI. In general, fluid's thermodynamic properties (specific heat at constant pressure C_p $(J/K/kg)$, gas constant R $(J/K/kg)$ and molecular weight M (kg/mol)) are obtained at each stage via weighted addition according to its chemical composition. Moreover, the effect of temperature on C_p is also considered by means of polynomials estimated via least-squares fitting by running *Cantera* off-line. Integration (automatic variable step with *ode23* or *ode45* method) is performed with lower saturation bounds, so as to avoid unphysical negative values in thermodynamic variables. Moreover, reverse flow is not considered before chambers and the shaft is supposed to turn in only one direction.

1) Transient effects considered and neglected: the following transient effects, which have a great impact on components' modelling approaches are taken into account: reverse flow and compressibility in chambers and turbines. Reverse flow is capital in some valves like VGC and some pipes like LTH in Vulcain, serving to distribute the flow among turbines. Compressibility is present in the components where the flow is gaseous and at high temperature, like combustion chambers and turbines. These do not include injection valves, where the flow is considered cold and hence liquid (or supercritical in the hydrogen case). Thus, there is no limitation on valves' choked mass flow.
Heat exchange has been studied after adding a simplified cooling circuit relating the main chamber and its hydrogen input flow. The effect of rising hydrogen's temperature is relevant but the amount of heat extracted from the chamber does not alter its internal fluid-dynamic equations.
Other effects which are also neglected are: water-hammer, turbomachines' stall and surge, combustion instabilities, chugging, cavitation and shockwaves. The water-hammer effect does not seem relevant in pump-fed engines, where it is assumed to be damped. Stall and surge are generally dealt with by means of operating constraints. Combustion instabilities are out of scope (modelling should get very precise). Thus, no injection delays are considered. Chugging physics comprises interactions between different complex phenomena (combustion delays, varying hydraulic impedances, transient thermal flows, etc.) and hence it is also out of scope. Cavitation in liquid lines, which might be relevant in valves and pumps, is neglected for simplification. Shockwaves within lines are assumed to be avoided by engine's design.

2) Conservation equations: the three main conservation equations used in this model have already been mentioned in the state of the art since they are the common ones for thermofluidic systems: mass (or continuity), momentum and energy conservation. Mass-conservation equation, applicable to capacitive elements like cavities, is:

$$\frac{d}{dt}(\rho V) = \dot{m}_{in} - \dot{m}_{out}, \tag{2}$$

where ρ is density (kg/m^3), V (m^3) is volume, and $\dot{m}$ is mass flow rate (kg/s). Momentum-conservation equation comes from the equilibrium of forces in a fluid line inside resistive elements [16], [17]:

$$\left(\frac{L}{A}\right)\frac{d\dot{m}}{dt} = p_{in} - p_{out} - k_{res}\dot{m}|\dot{m}|, \tag{3}$$

where L is length (m), A is area (m^2), p is pressure $(Pa$, or bar in figures) and k_{res} is the corresponding resistance coefficient $(1/kg/m)$. The quotient L/A is the inertia of the element. Finally, the energy-conservation equation is again applicable to capacitive elements [6]:

$$\frac{d}{dt}\left(\frac{pV}{\gamma - 1}\right) = (H_{in}\dot{m}_{in} - H_{out}\dot{m}_{out}) + \Phi, \tag{4}$$

γ being the specific heat ratio, H enthalpy (J/kg) and Φ (W) being the heat transferred through the walls (received or sent). These basic equations will serve to define the ordinary differential equations of the system in this paper.

3) Tanks: tanks are considered as a very simple component, just used to define the input flow vector to the engine as a function of the specified parameters (pump inlet pressure and temperature and type of propellant) and of the required mass flow, which is the sum of the calculated mass flows corresponding to line's downstream valves. A maximum mass output could be easily set but it is not of interest in this case.

4) Pumps: pumps modelling presents polynomials for pressure and torque. The polynomial for outlet pressure $p_{P,out}$ is the following:

$$p_{P,out} = p_{P,in} + a_{PrsP}\frac{\dot{m}_{in}^2}{\rho_P} + b_{PrsP}\cdot\omega\cdot\dot{m}_{in} + c_{PrsP}\cdot\rho_P\cdot\omega^2, \tag{5}$$

where ω is rotational speed (rad/s) and a_{PrsP}, b_{PrsP} and c_{PrsP} are the coefficients defining pump's pressure characteristic curve. The associated polynomial for torque Tq_P (Nm) is:

$$Tq_P = -\left|(a_{CplP}\frac{\dot{m}_{in}^2}{\rho_P} + b_{CplP}\cdot\omega\cdot\dot{m}_{in} + c_{CplP}\cdot\rho_P\cdot\omega^2)\right|, \tag{6}$$

where a_{CplP}, b_{CplP} and c_{CplP} define pump's torque characteristic curve. Equivalent expressions are proposed in [6], [12] and [17]. An important assumption made is the consideration that the inertial term of the liquid mass inside the pump is already included in line's overall inertial term, present in valves.

5) Pipes: a pipe represents a pressure drop due to friction. Some pipes, corresponding to pre-chambers lines, are considered static and without inertial term since the whole inertial term of the line is considered in downstream valves. In those cases, mass flow is imposed and output pressure is computed with the static pressure drop equation. Other pipes are considered dynamic (LTH in *Vulcain*), and hence output pressure is imposed and mass flow derivative is computed from the momentum-conservation equation (3). An additional non-reactive cavity (LTH) has to be placed before the hydrogen turbine for causality purposes.

6) Valves: valve components are dynamic resistive elements and hence present a differential equation on their mass flow (3). For simplification they contain chamber injectors too, since they are the last elements before chambers. An interpolation is performed so as to obtain a correlated value of valve's resistance according to the angle. In the case of the main chamber fuel valve (VCH in *Vulcain*), it also presents the resistance and inertia of the cooling circuit through which fuel must flow. Injectors are taken into account so as to consider the real back pressure, which is slightly higher than the input value corresponding to downstream chamber pressure. Indeed it is necessary that injectors produce a pressure drop so as to avoid reverse flow.

VGC butterfly valves: butterfly valves present basically the same dynamic formulation. There are only some differences in their resistance correlation to angle. In *Vulcain*, the VGC (hot gas valve) valve is of this kind and is used to establish the flow balance between turbines, and hence to tune the global mixture ratio. The flow directed to the oxidiser turbine is the one flowing through this valve. In order to avoid iterative loops and to ensure causality, an additional cavity has to be added downstream, whose pressure is considered as valve's outlet pressure.

7) Starter: this simple yet vital component computes starter output flow properties when GG's igniter flag is activated. Injected mass flow is a simple function of time and temperature T (K), C_p and R are supposed constant. Its outlet composition is ignored and neglected. The binary $ignit$ flag remains true after starter's activation.

8) Combustion chambers: not only the main combustion chamber (CC) but also the GG chamber are modelled via this dynamic component. Indeed, combustion chambers contain a sub-component, the cavity, which may be reactive (combustion possible) or not. The chamber component includes a combustion efficiency and always considers reactive cavities.

9) Cavities: this dynamic capacitive component is sometimes necessary between resistive components (valves, turbomachines, pipes) to render equation causal-implicit. In this model, apart from the reactive CC and GG cavities, two non-reactive cavities are included before turbines, after the LTH pipe and after the VGC valve.

First of all, injected fuel and oxidiser (if present) are merged in a simple way through a mass-flow-weighted addition. In the reactive case, mass production and consumption fractions of each species (μ_i) are computed statically as a function of mixture ratio, supposing that they stay constant at a given mixture ratio. This consist in a simplification of combustion kinetics, since the ARRHENIUS equations do not provide much more precision while highly increasing complexity. Here, the excess fuel or oxidiser, present at non-stoichiometric mixture ratios (almost always), is considered so as to establish the outlet composition (MR_{st} is the stoichiometric mixture ratio). If $MR \leq MR_{st}$ (unburned fuel):

$$\mu_{fu,in} = \frac{MR}{(MR+1)MR_{st}}\,(burned\,fuel\,fraction) \tag{7}$$

$$\mu_{fu,out} = \frac{1-\frac{MR}{MR_{st}}}{MR+1}\,(unburned\,fuel) \tag{8}$$

$$\mu_{ox,in} = \frac{MR}{MR+1} \tag{9}$$

$$\mu_{ox,out} = 0, \tag{10}$$

else (unburned oxidiser):

$$\mu_{fu,in} = \frac{1}{MR+1} \tag{11}$$

$$\mu_{fu,out} = 0 \tag{12}$$

$$\mu_{ox,in} = \frac{MR_{st}}{MR+1}\,(burned\,oxidiser\,fraction) \tag{13}$$

$$\mu_{ox,out} = \frac{MR-MR_{st}}{MR+1}\,(unburned\,oxidiser). \tag{14}$$

Combustion products' mass fractions μ are computed according to the propellant combination, which presents different reactions. In the *Vulcain* case LOX/LH_2 only presents water

vapour as a product. Hence, it will represent 100% of burned reactants. In LOX/LCH_4 engines, such as *Prometheus*, there is a proportion between water vapour and carbon dioxide. If ν represents the number of moles in the stoichiometric reaction and M molar masses, individual products mass fractions are:

$$\mu_{p,i} = \frac{\nu_i}{\nu_{total}} \frac{M_i}{M_{total}} (\mu_{fu,in} + \mu_{ox,in}), \tag{15}$$

after multiplying by the burned mass fraction, converted into products.

Then, cavity temperature T_c (of combustion or not) is computed by means of the gas equation of state, considering the composition at input (R_{in}) so as to include its physical relation to mixture ratio. As a simplification, combustion efficiency η_c is considered in that gas equation (1 in non-reactive cavities):

$$T_c = \frac{p_c}{R_{in}\rho_c}\eta_c. \tag{16}$$

Efficiency serves here as an empirical tool to represent the thermal losses associated to dissociations, diffusion and three-dimensional effects (among others), which are not modelled and which would reduce temperature in reality. An alternative simplification option could have been correcting C_p first, which is dependent on temperature. The influence of the pyrotechnic starter in GG flow properties is expressed via simple weighted additions, serving to update GG's inlet C_p, R and temperature. Output flow depends on the type of cavity. In the GG, mass flow through the throat is set equal to the sum of the flows through downstream VGC and LTH, but it is saturated to the choked flow [18]. In the CC and pre-turbine cavities, outlet static pressure is initially assumed as the ambient one and mass flow is computed subsonically until the throat chokes. In other words, until cavity's total pressure increases enough so as to obtain critical conditions at a higher pressure than ambient.

With this outlet mass flow, and assuming that the gas volume V_g is equal to cavity's one (could be improved with a gas volume differential equation [17], but it is neglected), the mass-conservation equation (2) can be set:

$$\frac{d\rho_c}{dt} = \frac{\dot{m}_{in} - \dot{m}_{out}}{V_g}. \tag{17}$$

In order to obtain all the terms of the energy-conservation equation, further computations have to be performed. As said before, species' production and consumption rates are assumed constant at a given mixture ratio (zero in non-reactive cavities). In the energy equation adapted to reactive cavities (20), there is a term representing mass variation rates of each species per unit of volume ($\dot{w}_i$). This is expressed for each reacting (r) and produced (p) species as:

$$\dot{w}_{r,i} = -\frac{\mu_{in,i}\dot{m}_{in}}{V_g}, \tag{18}$$

$$\dot{w}_{p,i} = \frac{\mu_{out,i}\dot{m}_{in}}{V_g}. \tag{19}$$

The energy equation expressed for pressure is the following, considering additional combustion terms, one inlet (propellant mixing ignored) and one outlet to the cavity and neglecting volume and efficiency variations and cooling [6]. The subscript i concerns all species while j only concerns the injected ones.

$$\begin{aligned}\frac{dp_c}{dt} = \frac{(\gamma_{out}-1)\dot{m}_{in}}{V_g}\Bigg(&\frac{\gamma_{in}p_c}{(\gamma_{in}-1)\rho_{in}} \\ &+ \frac{C_{v,in}p_c(\gamma_{in}-\gamma_{out})}{C_{v,out}\rho_c(\gamma_{out}-1)^2}\Bigg) \\ - \frac{p_c\gamma_{out}}{V_g\rho_c}\dot{m}_{out} - ignit\Bigg(&(\gamma_{out}-1)\sum_i(\dot{w}_i h_{f,i}) \\ - \frac{\gamma_{out}p_c}{(\gamma_{out}-1)\rho_c}\sum_i&\left(\left(\frac{C_{p,i}}{C_{p,out}} - \frac{C_{v,i}}{C_{v,out}}\right)\dot{w}_i\right) \\ &+ \frac{\gamma_{out}-1}{V_g}\sum_j(C_{p,out}T_{vap,j} - \\ (L_{v,j} + C_{p,j}(T_{vap,j} - T_{in,j})))\dot{m}_{in,j}&\Bigg),\end{aligned} \tag{20}$$

where $h_{f,i}$ is the formation enthalpy of each species (J/kg), C_v is specific heat at constant volume, $T_{vap,j}$ is the vaporisation or boiling temperature of each species and $L_{v,j}$ (J/kg) is the vaporisation heat of each species (considered positive since endothermic). The terms multiplied by $ignit$ are related to combustion and are only activated when the igniter/starter is on in reactive cavities. Vaporisation heat influence (last term in (20)) has been observed to be relevant in results.

10) Turbines: turbines are represented by a supersonic model valid above some given rotational speed and pressure ratio, similar to [12]. First, the reduced rotational speed N_R (non-dimensional, equivalent to a Mach number) is computed [12]:

$$N_R = \frac{\omega Rad_T}{\sqrt{\gamma R T_{T,in}}}, \tag{21}$$

Rad_T being turbine's radius (m). Temperature is taken from the previous integration step by means of a unit delay, in order to avoid an iterative loop. With this temperature, outlet pressure $p_{T,out}$ can be computed by supposing a choked nozzle [18]. Then, work W is calculated with the pressure ratio π_T (defined greater or equal than 1), all assuming that γ does not vary much from input to output:

$$W = \dot{m}\frac{\sqrt{\gamma R T_{t,in}}}{\gamma - 1}(1 - \pi_T^{\frac{1-\gamma}{\gamma}})Rad_T. \tag{22}$$

Next, a regression model with eight coefficients ($a_{T,1}$ to $a_{T,8}$) and an auxiliary correlating variable ($Corr$) is applied to obtain the specific torque ST and then efficiency:

$$\begin{aligned}ST = (a_{T,1} + N_R(a_{T,2} + N_R a_{T,3}) + \pi_T(a_{T,4} + \pi_T a_{T,5}) \\ + a_{T,6}\pi_T N_R + a_{T,7}\ln(\pi_T) + a_{T,8}\ln(N_R)) \cdot Corr.\end{aligned} \tag{23}$$

The previous correlation is not valid for too low pressure ratios or reduced rotational speeds. Hence, for lower values a

linear extrapolation is performed from $\pi_T = 1$ (by definition) and zero specific torque, as in [6]. Outlet temperature is easily obtained by the typical gas-turbine equation after having computed turbine's efficiency η_T:

$$\eta_T = ST \cdot N_R. \tag{24}$$

Finally, generated torque Tq_T is calculated [12]:

$$Tq_T = ST \cdot W. \tag{25}$$

11) Shafts: the shaft is a simple component containing the mechanical differential equation on its rotational speed ω:

$$\frac{d\omega}{dt} = \frac{Tq_T - Tq_P}{I_{TP}}, \tag{26}$$

where I_{TP} is shaft's angular inertia ($kg \cdot m^2/s$).

IV. Translation into a state-space model

The previous approach just consists in a component-wise thermodynamic modelling, conceived for simulation purposes. The goal of this second modelling phase is to obtain a global expression of the whole engine within a state-space model. For this sake, once the simulator started to reach design values (Table I), all components' models were joined by means of the symbolic computing environment *Maple*. In other words, basically the same equations from the previous Section III were associated according to *Vulcain* flow schematic. In this manner, a general expression of engine's transient behaviour could be obtained, in which some inter-component inputs and outputs are not present (the ones without differential equation). This expression consists in a set of nonlinear ODEs which is a function of only states (integrated variables), inputs (control action) and parameters (engine characteristics). For instance, pumps outlet pressures and temperatures do not appear because they are none of them. Although, some simplifications with respect to simulator's equations had to be performed so as to obtain globally-defined expressions. That is to say, equations which do not contain internal conditional or too complex statements distancing the model from the state-space formalism were modified. These simplifications, not altering to a relevant extent the transient behaviour of the system, consist in:

- All saturations in the previous thermodynamic equations were eliminated.
- Turbines: in order to eliminate the problematic output-temperature feedback with delay, the assumption of a zero ΔT was checked to be acceptable. In addition, this simplification also helps reduce the complexity related to the low-regime extrapolation.
- Piecewise-continuous equations based on conditional statements were rewritten into single equations by means of smooth approximations of the Heaviside function.

A further difference between both models, which actually complexifies the state-space one, is the translation of the mass-conservation equations in cavities. These differential equations concern densities in their most simple form. However, densities are generally not measured in rocket engines. That is the reason why they were re-expressed via the chain rule as functions of temperatures, which are generally measured.
Up from this point, the resulting system was analysed and checked to still be far too complex for deriving nonlinear control laws. Hence, a further list of simplifications was implemented. This reduces model fidelity during transients but eases the development of control algorithms, which will have to cope with this model mismatch. These modifications are:

- Two states, concerning temperatures in pre-turbine cavities, are assumed equal to T_{GG} with little error and hence eliminated from the state vector.
- Flow thermodynamic properties formally depend on state variables such as mass flow ratios and temperatures. This fact complexified to a great extent the model, introducing numerous nonlinearities. Thus, their values are considered constant. The ones depending on mixture ratios, like mixing outcome and variable mass fractions (e.g. (7) to (15)), are evaluated at their desired end values. Temperature-dependent ones are averaged along the transient phase.
- VGC resistance coefficient is considered equal to its design value, so as to avoid its polynomial angular dependency.
- After a numerical sensitivity analysis of all terms in equations, the ones presenting three orders of magnitude less than the rest were neglected. These correspond in general to terms associated to the squares of GG mass flows (small), to vaporisation heat in cavities, and to some state products in valves equations.
- The expressions of choked mass flow and turbine specific torque were rewritten into simplified first-order expressions via least-squares regression so as to avoid their highly nonlinear terms.
- Starter mass flow fraction was kept constant for simplifying its dependency on injected propellants mass flows.

After all the computations, this is the resulting nonlinear state-space model $\dot{x} = f(x, u_c, u_d)$, where $u_c \in [0, 90]^\circ$ is the vector of continuous inputs and $u_d \in \{0, 1\}$ is the vector of discrete inputs:

$$\begin{bmatrix} \dot{\omega}_H \\ \dot{\omega}_O \\ \dot{p}_{CC} \\ \dot{p}_{GG} \\ \dot{p}_{VGC} \\ \dot{p}_{LTH} \\ \dot{T}_{CC} \\ \dot{T}_{GG} \\ \ddot{m}_{VCH} \\ \ddot{m}_{VGH} \\ \ddot{m}_{VCO} \\ \ddot{m}_{VGO} \\ \ddot{m}_{VGC} \\ \ddot{m}_{LTH} \end{bmatrix} = f \left(\begin{bmatrix} \omega_H \\ \omega_O \\ p_{CC} \\ p_{GG} \\ p_{VGC} \\ p_{LTH} \\ T_{CC} \\ T_{GG} \\ \dot{m}_{VCH} \\ \dot{m}_{VGH} \\ \dot{m}_{VCO} \\ \dot{m}_{VGO} \\ \dot{m}_{VGC} \\ \dot{m}_{LTH} \end{bmatrix}, \begin{bmatrix} \alpha_{VCH} \\ \alpha_{VGH} \\ \alpha_{VCO} \\ \alpha_{VGO} \\ \alpha_{VGC} \end{bmatrix}, \begin{bmatrix} i_{CC} \\ i_{GG} \end{bmatrix} \right), \tag{27}$$

which makes a total of fourteen states: two shaft rotational speeds, four cavity pressures, two cavity temperatures and six

valve and pipe mass flow rates. Inputs to the system are the five continuous valve opening angles and the two discrete activations of igniters or starters. The details of the equations are not shown due to their relatively high complexity and to the lack of space. Some physical and operating constraints have to be set on states:

$$\omega_i > 0;\ p_i > 0;\ T_i \geq 20K. \tag{28}$$

V. Analysis of Results

The most interesting transient phase to simulate is the start-up of the engine, whose event sequence has been kept identical at all cases:

1) VCH opens at $t_{VCH} = 0.1s$ (fuel-lead approach).
2) VCO opens at $t_{VCO} = 0.6s$.
3) Main chamber ignition i_{CC} at $t_{i_{CC}} = 1s$.
4) Starter activates at $t_{i_{GG}} = 1.1s$. It provides full flow during $0.8s$ and half flow during $0.55s$ more.
5) VGH and VGO open some ds later.

The following results consist then in the open-loop behaviour of the system, since no controller is imposed yet. Constant opening angles are fed to valves, related to engine's steady-state: $\alpha_{VCH} = \alpha_{VCO} = 90°$, $\alpha_{VGH} = 72°$, $\alpha_{VGO} = 48°$ and $\alpha_{VGC} = 57°$. Initial conditions for pressure are ambient ones (start on ground) and for mass flows are almost zero (10^{-15}), as logical in a start-up. Regarding shaft speeds, the model does not numerically allow starting at zero. Thus, they start at $2.05rpm$ for hydrogen and $1.29rpm$ for oxygen, what already establishes the ratio between shafts. Temperatures start at $20K$ in the hydrogen line and at $90K$ in the oxygen one because prior to start-up there is always a procedure of chill-down, in order to minimise thermal shocks and avoid cavitation before pumps.

A. Simulator

Concerning the thermo-fluid-dynamic simulator, fig. 2 depicts its results in open loop during the first 4s of start-up operation. The figure shows results of chambers pressures (a), mixture ratios (b), mass flows through valves (c), chambers temperatures (d) and shaft rotational speeds (e). All ordinate values are intentionally not depicted. Transient behaviour matches the expected results in general. Starter activation and the subsequent opening of GG valves can be clearly observed in the evolution of GG pressure. Besides, steady-state values, attained after 2.75s approximately, are close to design ones (Table I), acceptable for an open-loop simulation. Mixture ratio starts to be meaningful up from 1.75s of simulation, where all valves are open and the starter is ending its contribution. From its definition, if the corresponding hydrogen flow becomes zero, the ratio tends to infinity, which happens during that interval after starter activation.

B. State-space model

Moving on to the state-space model, its results are also satisfactory and close to the previous ones, as depicted in fig. 3. The influence of simplifications (listed in Section IV) results in some differences in final values and especially in transient values. Concretely, pressures are somewhat over-quantified during transients (until +20%) but reach accurate final values. Mixture ratios are slightly over-quantified in their final value (+7%), resulting from variations in mass flow (between -4% and +4%). Temperature transient behaviour is not well predicted with this model, mainly because its effect on parameters has been averaged. CC dynamics are too fast, but adequate final values are attained.

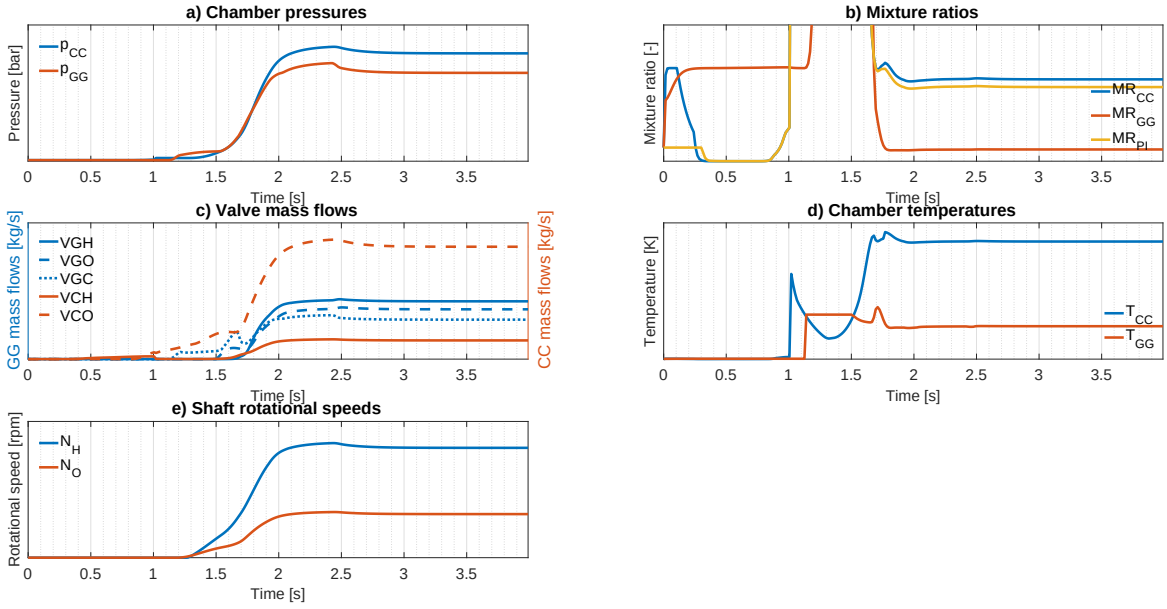

Fig. 2. Vulcain T-RETM simulator results at start-up during 4s

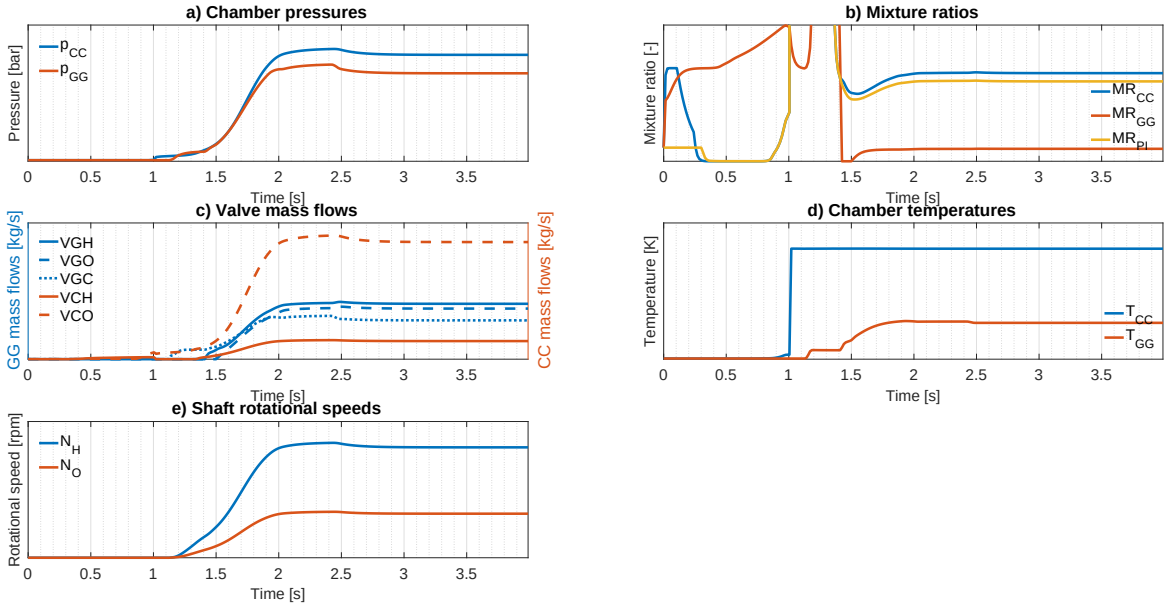

Fig. 3. Vulcain T-RETM state-space results at start-up during 4s

Some throttling scenarios have been simulated, in which valve's opening angles are increased and decreased. The same simulation sequence has been set for the GG and VGC cases: the first five seconds are nominal, then there are $7.5s$ of $\Delta\alpha = +15°$, $7.5s$ of $\Delta\alpha = -15°$ (with respect to nominal) and finally other $5s$ of nominal behaviour. The effects of each type of valves (GG, VGC and CC) have been tested separately. Fig. 4 depicts throttling by adjusting GG valves. It seems clear that these valves are directly related to chamber pressure and hence to thrust, the variable to control in the end. Throttling results by adjusting the VGC valve are not shown due to the lack of space. It can be affirmed that this valve influences mixture ratio to a greater extent, because it is indeed used to distribute the flow between turbines. Concerning CC valves, they are not depicted since they do not serve to control any of the important variables in a practical way. Thus, it will only be useful to operate them with bang-bang logics.

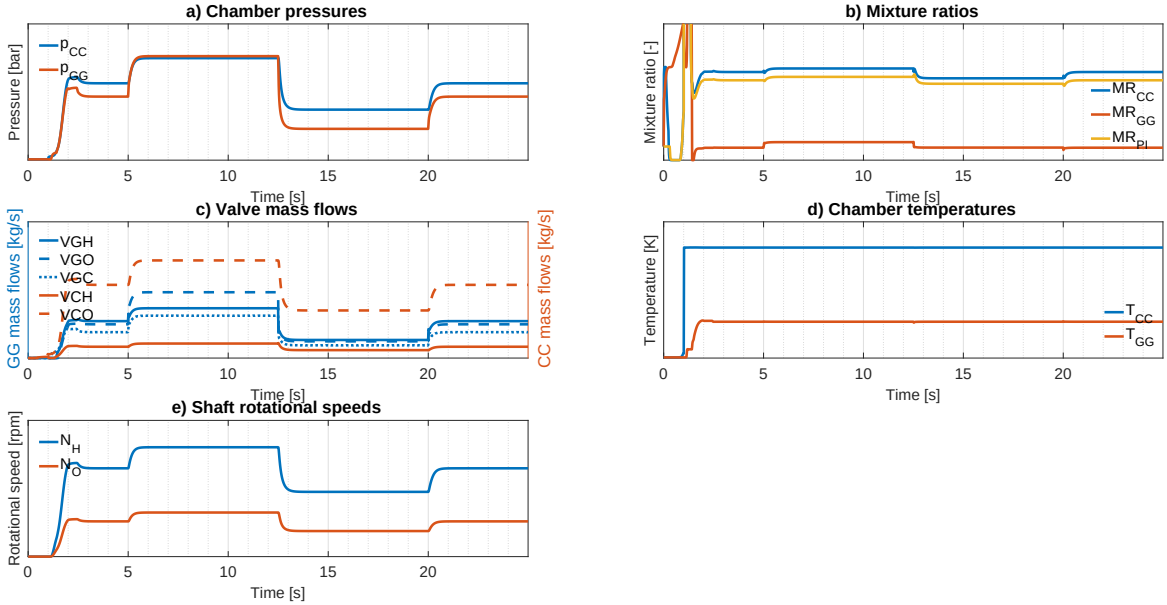

Fig. 4. Vulcain T-RETM state-space throttling results by adjusting GG valves

VI. Conclusion

The evolving operating requirements of pump-fed rocket engines, currently related to reusability scenarios, force the improvement of their control algorithm. The first steps in this new control loop have been tackled in this paper, where a nonlinear state-space model representative of the *Vulcain* engine, a gas-generator cycle, has been derived. The process to obtain that model adapted to the control formalism begun with a thermo-fluid-dynamic modelling phase based on conservation equations on mass, momentum and energy. These typical thermodynamic equations are applied to each basic component of a rocket engine, like valves, combustion chambers or turbopumps. These components are then joined to build a simulator of the engine, which satisfactorily predicts the start-up transient of the engine. Transient phases are indeed the main focus of the future control algorithm, since they are nowadays carried out in open loop. Subsequently, the same system was translated into a symbolic model, so as to obtain the formal nonlinear differential equations as functions of states, inputs and engine parameters. States comprise rotational speeds, pressures, temperatures and mass flows. Some inputs are continuous (valves angles) and others are discrete (igniter and starter), which renders the system hybrid. An acceptable agreement between results from both types of model is attained. Hence, the state-space model will be used in the upcoming controller design. The analysis of its dynamic characteristics show good controllability of thrust through the gas-generator injection valves, and of mixture ratio through the turbines' flow-distribution valve.

References

[1] Le Gonidec S., "Automatic & Control applications in the European space propulsion domain. From need expression to preparation for an uncertain future. ACD2016 Airbus Safran Launchers, Lille, France," 2016.

[2] Duyar A., Ten-Huei G., and Merrill W.C., "Space shuttle main engine model identification," *IEEE Control Systems Magazine*, vol. 10, no. 4, pp. 59–65, 1990.

[3] Raposo H., "Mixture ratio and thrust control of a liquid-propellant rocket engine," Master's thesis, ISAE-Supaero, Instituto Superior Tecnico, CNES, 2016.

[4] Lorenzo C.F., Ray A., and Holmes M.S., "Nonlinear control of a reusable rocket engine for life extension," *Journal of Propulsion and Power*, vol. 17, no. 5, pp. 998–1004, 2001.

[5] Dai X. and Ray A., "Damage-Mitigating Control of a Reusable Rocket Engine: Part IIFormulation of an Optimal Policy," *Journal of Dynamic Systems, Measurement, and Control*, vol. 118, pp. 409–415, Sept. 1996.

[6] Ordonneau G., Masse J., and Albano G., "CARINS: Un logiciel de modelisation et de simulation pour les procedes industriels complexes fonde sur des logiciels libres," *REE: Revue de l'Electricite et de l'Electronique*, vol. N. 4, 2006.

[7] Lorenzo C.F. and Musgrave J.L., "Overview of rocket engine control," in *AIP Conference Proceedings*, vol. 246, pp. 446–455, AIP, 1992.

[8] Nassirharand A. and Karimi H., "Mixture ratio control of liquid propellant engines," *Aircraft Engineering and Aerospace Technology*, vol. 77, pp. 236–242, June 2005.

[9] Santana A. and Goes L.C.S., "Design and dynamic characteristics of a liquid-propellant thrust chamber," 1999.

[10] Santana A. and Goes L.C.S., "Dynamic modeling and stability analysis of a liquid rocket engine," in *15th Brazilian Congress of Mechanical Engineering COBEM*, (Sao Paulo, Brazil), Centro Tecnico Aeroespacial, IAE/CTA, 1999.

[11] Musgrave J.L., Guo T.H., Wong E., and Duyar A., "Real-time accommodation of actuator faults on a reusable rocket engine," *IEEE transactions on control systems technology*, vol. 5, no. 1, pp. 100–109, 1996.

[12] Iffly A. and Brixhe M., "Performance Model of the Vulcain Ariane 5 Main Engine," in *35th AIAA/ASME/SAE/ASEE Joint Propulsion Conference and Exhibit*, vol. AIAA 99-2472, (Los Angeles, USA), AIAA, 1999.

[13] Zhang Y.L., "State-space analysis of the dynamic characteristics of a variable thrust liquid propellant rocket engine," *Acta Astronautica*, vol. 11, pp. 535–541, July 1984.

[14] Chapman J.W., Lavelle T.M., May R.D., Litt J.S., and Guo T.H., "Propulsion System Simulation Using the Toolbox for the Modeling and Analysis of Thermodynamic Systems (T MATS)," in *Propulsion and energy forum in 50th AIAA/ASME/SAE/ASEE Joint Propulsion Conference*, vol. 2014-3929, (Cleveland, USA), AIAA, July 2014.

[15] Lavelle T.M., Chapman J.W., May R.D., Litt J.S., and Guo T.H., "Cantera Integration with the Toolbox for Modeling and Analysis of Thermodynamic Systems (T-MATS)," in *AIAA/ASME/SAE/ASEE Joint Propulsion Conference*, (Cleveland, USA), July 2014.

[16] Lozano-Tovar P.C., "Dynamic models for liquid rocket engines with health monitoring application," Master's thesis, Massachusetts Institute of Technology, MIT Boston, 1998.

[17] Manfletti C., *Transient behaviour modelling of liquid rocket engine components*, vol. PhD Thesis 2009 of *Berichte aus der Luft- und Raumfahrttechnik*. Aachen: Shaker Verlag, 2010. OCLC: 685183465.

[18] Ruth E., Ahn H., Baker R., and Brosmer M., "Advanced liquid rocket engine transient model," in *26th Joint Propulsion Conference*, (Orlando, USA), American Institute of Aeronautics and Astronautics, 1990.